PAPER

Rapid synthesis of few-layer graphdiyne using radio frequency heating and its application for dendrite-free zinc anodes

View the article online for updates and enhancements.

2D Materials

Rapid synthesis of few-layer graphdiyne using radio frequency heating and its application for dendrite-free zinc anodes

Chen Yin[1,2,5], Miao Zhu[3,5], Ya Kong[2], Qian Wang[3,4], Henghui Zhou[3,4], Limin Qi[3,*] ![ORCID], Lianming Tong[2,*] ![ORCID]
and Jin Zhang[2,*] ![ORCID]

1 Academy for Advanced Interdisciplinary Studies, Peking University, Beijing 100871, People's Republic of China
2 Center for Nanochemistry, Beijing Science and Engineering Center for Nanocarbons, Beijing National Laboratory for Molecular Sciences, College of Chemistry and Molecular Engineering, Peking University, Beijing 100871, People's Republic of China
3 Beijing National Laboratory for Molecular Sciences, College of Chemistry and Molecular Engineering, Peking University, Beijing 100871, People's Republic of China
4 Beijing Engineering Research Center of Power Lithium-Ion Battery, Beijing 102202, People's Republic of China
5 Contributed equally to this work.
* Authors to whom any correspondence should be addressed.

E-mail: liminqi@pku.edu.cn, tonglm@pku.edu.cn and jinzhang@pku.edu.cn

Abstract

Graphdiyne (GDY), with specific configuration of sp- and sp^2-hybridized carbon atoms, is a kind of two-dimensional carbon allotrope. A series of approaches have been developed to synthesisze thin films of GDY, however, the controlled synthesis of GDY films on arbitrary metal substrates with good crystallinity still remains challenging. Herein, we propose an approach for the synthesis of few-layered GDY on arbitary metal substrate using a radio frequency (RF) heating directed temperature gradient at solid/liquid interface. RF irradiation only heats the metal substrate but not the solvent, thus the cross-coupling reaction occurs on metal substrate and monomers remain stable in the bulk solution. We obtained GDY film with homogenous morphology and an average thickness of 1–2 nm on the surface of metal substrate. Due to the high electrical conductivity and uniform pore size, GDY film is used as an artificial interface layer to avoid the formation of Zn dendrite in Zn ion batteries by direct synthesis on Zn anodes. The lifespan of symmetric cells is extended to more than 2000 h.

1. Introduction

Different from fullerene, carbon nanotubes and graphene [1–3], graphdiyne (GDY) is composed of sp- and sp^2-hybridized carbon atoms arranged in two-dimension (2D) [4, 5]. Since its discovery, GDY has shown significant potential applications in many fields due to its unique structures of diacetylenic linkages, well-distributed pores and large π-conjugated systems [6–18]. In 2010, Li *et al* proposed the first experimental method to synthesize GDY on copper substrate via *in situ* Glaser coupling reaction [19]. In 2018, Zhang *et al* proposed a van der Waals epitaxial method to synthesize triple-layered GDY film with ABC-stacking on graphene in a solution phase [20]. In 2020, they also developed a method using microwave-induced temperature gradient to synthesize thin films of GDY on the surface of

NaCl crystal, where the hexaethynylbenzene (HEB) monomers remain stable in cold solution and react at the hot interface [21]. However, the synthesis of few-layer GDY films with large area on arbitrary metal substrates still remain great challenge.

Herein, we proposed an approach for the synthesis of large area few-layered GDY on arbitrary metal substrates using radio frequency (RF) heating. We chose metal foils (Cu, Ag, and Au) as solid substrate, which can be heated by RF generator, and ethyl acetate as the solvent. RF irradiation only heats the metal substrate but not the solvent, thus monomers only react on the metal substrate. As a result, a thin film of GDY with an average thickness of 1–2 nm and a size as large as the substrate can be obtained. Transmission electron microscopy (TEM) characterization confirmed GDY films with good crystallinity. We prepared GDY directly on commercial Zn

plate to build Zn-GDY electrode, avoiding the damage and contamination caused by the transfer process. Due to the existance of GDY, at a high current of 20 mA cm^{-2}, the Coulombic efficiency (CE) of Zn-GDY electrode is over 98% for nearly 200 cycle. The symmetric cells with Zn-GDY reached a months-level lifespans of over 2400 h.

2. Disscusion

Figure 1(a) shows the schematic diagram of the synthetic processes. Briefly, 30 mg hexakis [(trimethyl-silyl)ethynyl] benzene (TMS-HEB) were dissolved into 50 ml ethyl acetate. One milliliter tetrabutylammonium fluoride (1 M in tetrahydrofuran) was added into the TMS-HEB solution. Under an argon atmosphere, the above solution was stirred at 0 °C for 15 min. Then, hexakisbenzene (HEB) was obtained and immediately used as the precursor for the coupling reaction. Twenty milligrams copper acetate were dissolved into 20 ml pyridine as the catalyst solution. Then, metal foil and 2 ml catalyst solution were added into the 15 ml precursor solution in a 50 ml beaker. The beaker was transferred in a RF generator. Under the RF irradiation for 5 min, the metal foil was heated and the temperature of solvent was kept low. A thin GDY film was obtained on the surface of metal foil. Figure S1 (available online at stacks.iop.org/2DM/8/044003/mmedia) shows the optical microscopy (OM) images of the GDY on Ag, Cu, and Au foils, and in figures 1(b)–(d), the scanning electron microscopy (SEM) images show smooth and homogeneous morphology of GDY films. The as-grown films can be easily transferred from the substrate onto arbitrary substrates using a poly(methyl methacrylate)-mediated technique for characterization and application. Figures S2–S4 show the OM, SEM images, and Raman scattering spectra of GDY films grown on different substrates transferred onto SiO$_2$/Si substrate. The typical thickness of the films shown by atomic force microscopy (AFM) images were about 1–2 nm (figures 1(e)–(g)).

The TEM image of GDY transferred onto a copper grid in low magnification shows free standing films of GDY (figures 2(a)–(c)). The high resolution TEM (HRTEM) images also show lattice fringes which are in good agreement with theoretical results of about 0.470–0.480 nm (figures 2(d)–(f)) [11]. Energy-dispersive spectroscopy (EDS) mapping results exhibit that the major element was carbon in obtained GDY films in figure S5. The inevitable defects might cause the existence of oxygen, the copper might come from the residual catalyst, and the silicon might come from the residue of HEB preparing process. Raman spectroscopy and x-ray photoelectron spectroscopy (XPS) further revealed the bonding structure and elemental composition. As shown in figure 2(g), the peak at 2176.2 cm^{-1} indicated
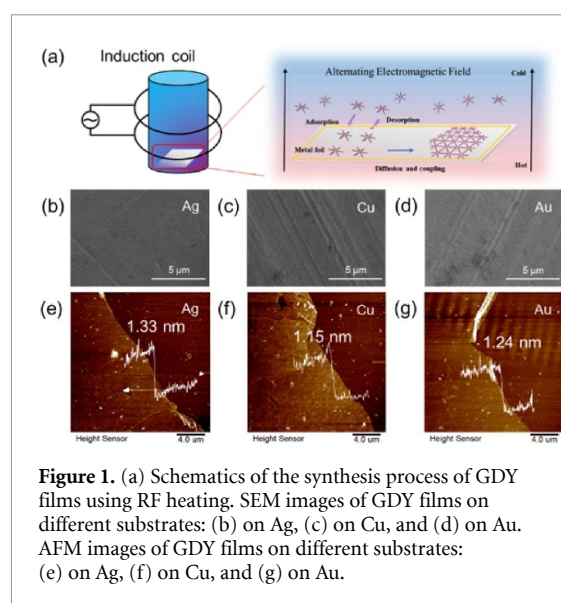

Figure 1. (a) Schematics of the synthesis process of GDY films using RF heating. SEM images of GDY films on different substrates: (b) on Ag, (c) on Cu, and (d) on Au. AFM images of GDY films on different substrates: (e) on Ag, (f) on Cu, and (g) on Au.

the successful coupling of monomers [19]. The XPS spectra of GDY on Cu substrate in figures 2(h) and (i) confirm the same result with EDS mapping. In figure 2(i), three subpeaks can be deconvoluted from the peak of C 1s, corresponding to *sp* hybridized carbon atoms (C≡C) at binding energies of 284.6 eV, sp^2 hybridized carbon atoms (benzene rings) at 285.2 eV, C–O at 286.5 eV, and C=O at 288.3 eV, respectively [22].

To understand the effect of the temperature gradient, we homogeneously heated the reaction system without RF irradiation for comparison. No GDY film but some carbon powder were found on Cu foil when the reaction system was heated to 80 °C by oil bath rather than RF irradiation (figure S6(a)). No distinct peak of coupled alkyne bonds was observed in Raman spectrum (figure S6(b)). The photograph (figure S6(c)) and Raman scattering spectra (figure S6(d)) of the solution after reaction completing shows that no GDY formed in bulk solution. These results indicate that RF heating directed temperature gradient solid/liquid interface is necessary for the growth and quality promotion of GDY. We can also controll the thickness of GDY films by adjusting Cu^{2+} concentration. As the AFM images shown in figure S7, the thickness of GDY film can be increased to more than 4 nm as the Cu^{2+} addition goes up to 0.25 mg. The Raman spectra in figure S7(d) exhibit the peak of conjugated diyne at 2177.6 cm^{-1} of GDY films with different thickness.

Besides 2D metal foil, GDY film can also be synthesized on metal substrates with different morphologies. We choose Ag nanowire and Au nanorod as the substrate and successfully synthesize GDY films on them. As shown in figures S8(a) and (b), the morphology characterization of Ag nanowire@GDY exhibits that few-layered GDY films was grown on Ag nanowire. And the Raman spectra in figure S8(c)
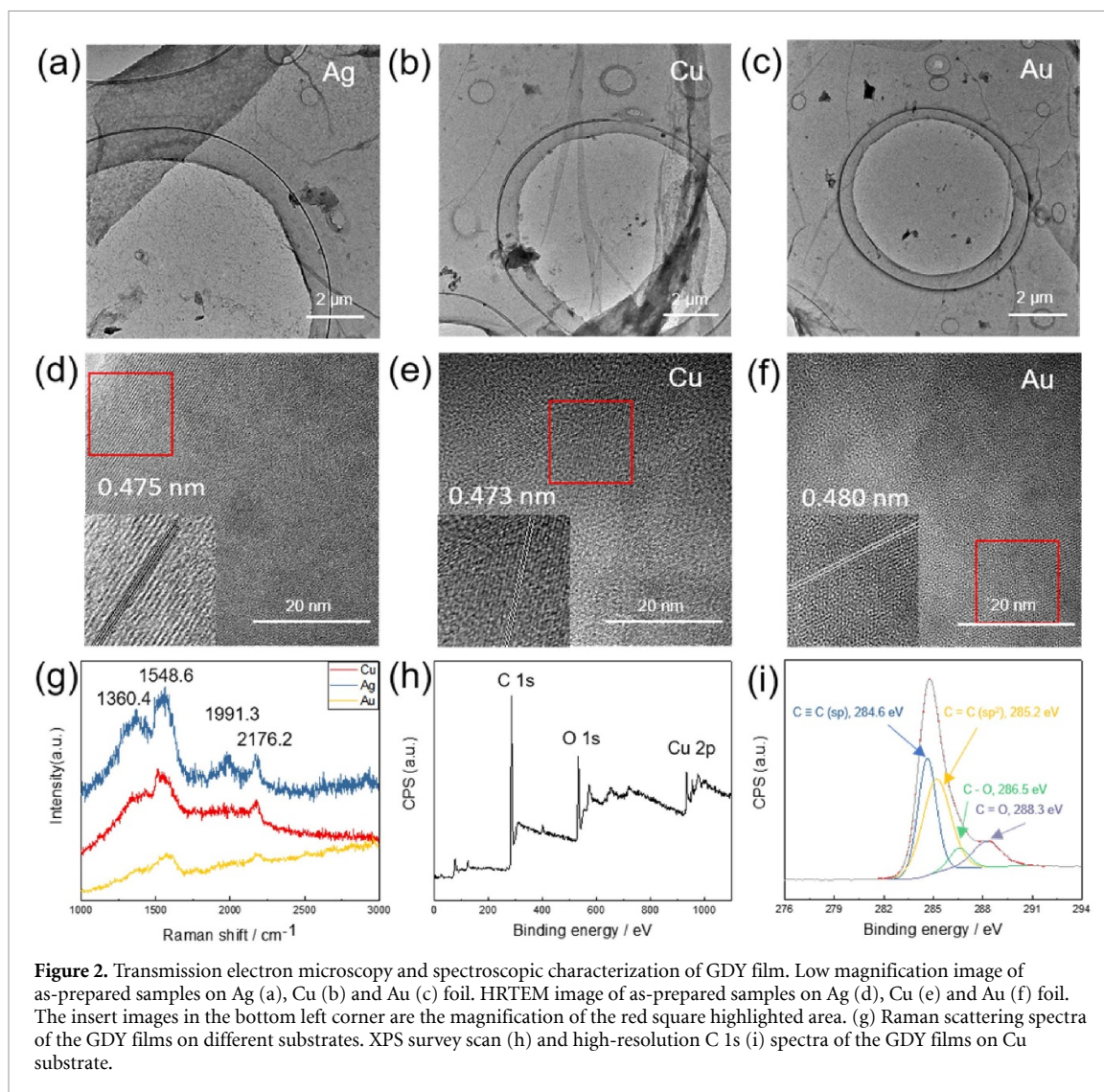
Figure 2. Transmission electron microscopy and spectroscopic characterization of GDY film. Low magnification image of as-prepared samples on Ag (a), Cu (b) and Au (c) foil. HRTEM image of as-prepared samples on Ag (d), Cu (e) and Au (f) foil. The insert images in the bottom left corner are the magnification of the red square highlighted area. (g) Raman scattering spectra of the GDY films on different substrates. XPS survey scan (h) and high-resolution C 1s (i) spectra of the GDY films on Cu substrate.

exhibit the peak of conjugated diyne at 2177.6 cm^{-1}. The similar results of Au nanorod@GDY are shown in figures S8(d)–(f).

Since GDY films with uniform continuity can be obtained via a RF heating on arbitrary metal substrate, it can be directly used for applications where metal substrate is a functional component, for example, as metal anode in batteries. This approach avoids the transfer process which usually causes damage and contamination of the samples. In recent years, Zn-ion batteries (ZIBs) as promising energy storage devices have attracted wide attention. However, the formation of Zn dendrites still impedes the commercialization of aqueous ZIBs, and reduces their safety, reversible capacity, and discharging platform potentials [23–27]. The formation of Zn dendrites is mainly due to the fragile solid electrolyte interface (SEI) and huge volume expansion/shrink during Zn stripping/plating cycles, which lead to additional SEI layers and newly exposed Zn surface. These two factors disturb the electric-field distribution greatly and in turn cause the uneven Zn deposition [28–30]. Therefore, reassessing the performance of the existing

dendrite protection strategies under the condition of large anode loading mass is necessary.

GDY film was directly grown on Zn electrode (denoted as Zn-GDY) using our RF heating method, with the purpose of fundamentally eliminating Zn dendrite by redistributing the Zn^{2+} concentration field. This interface modification of Zn plate has undergone an evolution of color from silver to deep yellow, which means successfully integrating GDY onto the Zn plate (figure 3(a)). SEM images of two kinds of electrodes show that the surface of Zn-GDY electrode is flatter and smoother than pure Zn electrode (figure S9). Hydrophilicity of Zn electrodes before and after GDY modification are shown in figure 3(b). Contact angle decreases from 105° for pure Zn electrode to 43° for Zn-GDY, demonstrating a remarkable improvement of interfacial hydrophilicity. According to the given testing procedure, the CE of the Cu/Zn and Cu/Zn-GDY electrodes were measured [31]. The Zn plating/stripping CE of Zn and Zn-GDY electrodes were further compared at the capacity of 2 mAh cm^{-2}. The CE of Zn-GDY electrode is over 98% at 2 mA cm^{-2}, 5 mA cm^{-2},
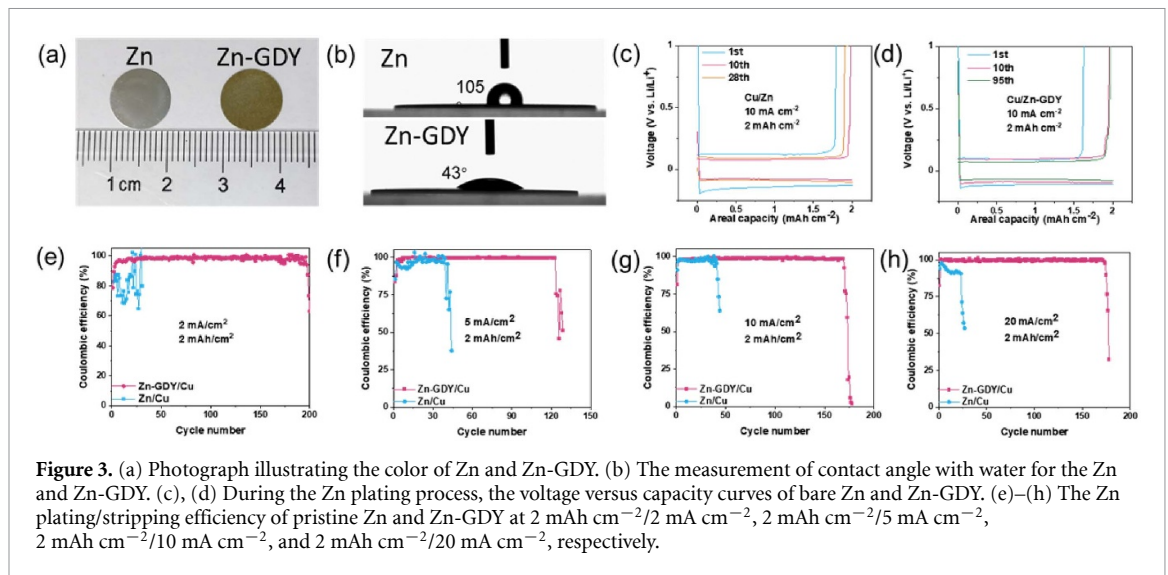
Figure 3. (a) Photograph illustrating the color of Zn and Zn-GDY. (b) The measurement of contact angle with water for the Zn and Zn-GDY. (c), (d) During the Zn plating process, the voltage versus capacity curves of bare Zn and Zn-GDY. (e)–(h) The Zn plating/stripping efficiency of pristine Zn and Zn-GDY at 2 mAh cm^{-2}/2 mA cm^{-2}, 2 mAh cm^{-2}/5 mA cm^{-2}, 2 mAh cm^{-2}/10 mA cm^{-2}, and 2 mAh cm^{-2}/20 mA cm^{-2}, respectively.

10 mA cm^{-2}, and 20 mA cm^{-2} for nearly 200 cycles (figures 3(e)–(h)). On the contrary, the CE of bare Zn electrode drops to below 70.0% after about 50 cycles. Figure 3(c) and d show the voltage versus capacity profiles of Zn and Zn-GDY electrodes with different cycles at 10 mAh cm^{-2}/2 mA cm^{-2}, respectively. In figure 3(d), apparently after 95 cycles, the Zn-GDY electrode exhibits almost the same charge/discharge profiles without obvious capacity fading (figure 3(g)). In contrast, at the 28th cycle the bare Zn electrode shows a significant distorted charge profile and lower charge capacity (figure 3(c)). After long-term cycling, the growth of Zn dendrite leads to the capacity attenuation of the Zn electrode. Besides, Zn-GDY electrode provides a lower nucleation overpotential, confirming the favorable Zn nucleation and plating on GDY surface to get a high CE and a uniform surface.

At 4 mA cm^{-2} and 4 mAh cm^{-2}, the short lifespan of nearly 80 h was caused by the Zn dendrites formation of Zn/Zn symmetric cells (figure 4(a)). On the contrary, Zn-GDY electrode established an ultralong lifespan of over 400 h at 4 mA cm^{-2}/4 mAh cm^{-2}. The following change of current density (4 mA cm^{-2}/2 mAh cm^{-2} and 2 mA cm^{-2}/2 mAh cm^{-2}) witnessed the longer lifespan (more than 2000 h). In figures 4(b)–(d), during the long-term cycling, the enlarged profiles in different time slots (5th, 100th and 200th) further demonstrate the stable voltage hysteresis of the Zn-GDY electrode. The results confirm that the coverage of GDY on Zn electrode indeed imporved the electrochemical stripping/plating behavior. Besides the electrical conductivity of GDY, the improvement of the hydrophilicity of the electrode also contributes to the migration of Zn^{2+} and the redistribution of the Zn^{2+} concentration field, leading to the elimination of the Zn dendrites (figure S10).

In summary, an approach to rapidly synthesize ultrathin GDY films on arbitrary metal substrate
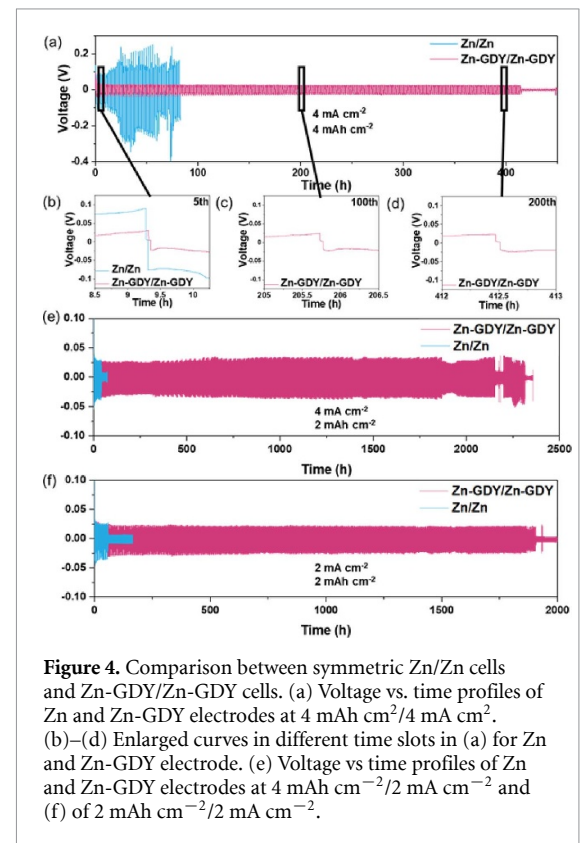

Figure 4. Comparison between symmetric Zn/Zn cells and Zn-GDY/Zn-GDY cells. (a) Voltage vs. time profiles of Zn and Zn-GDY electrodes at 4 mAh cm^2/4 mA cm^2. (b)–(d) Enlarged curves in different time slots in (a) for Zn and Zn-GDY electrode. (e) Voltage vs time profiles of Zn and Zn-GDY electrodes at 4 mAh cm^{-2}/2 mA cm^{-2} and (f) of 2 mAh cm^{-2}/2 mA cm^{-2}.

at a RF heating is developed. The reaction was controlled to occur only on metal substrate with high temperature and GDY films with thickness of 1–2 nm and good crystallinity were obtained. In order to redistribute the Zn^{2+} concentration, GDY artificial interface layer was integrated with commercial Zn plate. Symmetric Zn-GDY cells reached lifespans of several months over 2400 h, which extremely bridged the gap between laboratory study and practical use. This work paves a way for synthesis of GDY thin films on metal substrates, and by growing GDY film on metal anode, advances

the development of dendrite protection in electric cells.

3. Experimental section

3.1. Characterization
The prepared samples were characterized using SEM (Hitachi S-4800, accelerating voltage 1.0 kV), TEM (FEI Tecnai F30, acceleration voltage 300 kV), Raman spectroscopy (Horiba Jobin Yvon Lab-RAM HR 800, 532 nm), and XPS (Kratos Analytical Axis-Ultra spectrometer with Al Kα x-ray radiation).

3.2. Battery preparation
Symmetric batteries used two pieces of commercial Zn or Zn-GDY as electrodes. 3 M $Zn(CF_3SO_3)_2$ solution was used without any additives throughout the whole work while the separator is glassfiber film. These battery parts were assembled in coin-type cell (CR2032) to fabricate the batteries.

3.3. Electrochemical measurements
CV curves recorded at 2–20 mV s^{-1} were tested by electrochemical workstation (CHI 660). Rate capability and cycling performance under galvanostatic charge/discharge mode were examined on LAND test system. The voltage-time profiles of symmetric batteries were evaluated at varied current densities of 2–4 mA cm^{-2} with an areal capacity of 2–4 mAh cm^{-2}.

Data availability statement

All data that support the findings of this study are included within the article (and any supplementary files).

Conflict of interest

The authors declare no competing financial interest.

ORCID iDs

Limin Qi ⓘ https://orcid.org/0000-0003-4959-6928
Lianming Tong ⓘ https://orcid.org/0000-0001-7771-4077
Jin Zhang ⓘ https://orcid.org/0000-0003-3731-8859

References

[1] Kroto H W, Heath J R, O'Brien S C, Curl R F and Smalley R E 1985 *Nature* **318** 162
[2] Iijima S 1991 *Nature* **354** 56
[3] Novoselov K S, Geim A K, Morozov S V, Jiang D, Zhang Y, Dubonos S V, Grigorieva I V and Firsov A A 2004 *Science* **306** 666–9
[4] Baughman R H, Eckhardt H and Kertesz M 1987 *J. Chem. Phys.* **87** 6687–99
[5] Haley M M, Brand S C and Pak J J 1997 *Angew. Chem., Int. Ed.* **36** 836
[6] Li Y, Xu L, Liu H and Li Y 2014 *Chem. Soc. Rev.* **43** 2572–86
[7] Srinivasu K and Ghosh S K 2012 *J. Phys. Chem.* C **116** 5951–6
[8] Narita N, Nagai S, Suzuki S and Nakao K 1998 *Phys. Rev. B* **58** 11009
[9] Enyashin A N and Ivanovskii A L 2011 *Phys. Status Solidi* b **248** 1879–83
[10] Luo G *et al* 2011 *Phys. Rev. B* **84** 075439
[11] Long M, Tang L, Wang D, Li Y and Shuai Z 2011 *ACS Nano* **5** 2593–600
[12] Gao X, Zhou J, Du R, Xie Z, Deng S, Liu R, Liu Z and Zhang J 2016 *Adv. Mater.* **28** 168–73
[13] Li J, Gao X, Liu B, Feng Q, Li X B, Huang M Y, Liu Z, Zhang J, Tung C H and Wu L Z 2016 *J. Am. Chem. Soc.* **138** 3954–7
[14] Huang C, Zhang S, Liu H, Li Y, Cui G and Li Y 2015 *Nano Energy* **11** 481–9
[15] Feng Z, Li Y, Tang Y, Chen W, Li R, Ma Y and Dai X 2020 *J. Mater. Sci.* **55** 8220–30
[16] Feng Z, Tang Y, Chen W, Li Y, Li R, Ma Y and Dai X 2020 *Phys. Chem. Chem. Phys.* **22** 9216–24
[17] Fang Y *et al* 2020 *Angew. Chem., Int. Ed.* **59** 13021–7
[18] Fang Y, Xue Y, Hui L, Yu H and Li Y 2021 *Angew. Chem., Int. Ed.* **60** 3170–4
[19] Li G, Li Y, Liu H, Guo Y, Li Y and Zhu D 2010 *Chem. Commun.* **46** 3256–8
[20] Gao X *et al* 2018 *Sci. Adv.* **4** eaat6378
[21] Yin C, Li J, Li T, Yu Y, Kong Y, Gao P, Peng H, Tong L and Zhang J 2020 *Adv. Funct. Mater.* **30** 2001396
[22] Ferrari A C *et al* 2006 *Phys. Rev. Lett.* **97** 187401
[23] Zheng J *et al* 2019 *Science* **366** 645
[24] Yang Q, Mo F, Liu Z, Ma L, Li X, Fang D, Chen S, Zhang S and Zhi C 2019 *Adv. Mater.* **31** 1901521
[25] Wan F, Zhang L, Dai X, Wang X, Niu Z and Chen J 2018 *Nat. Commun.* **9** 1656
[26] Li M, Meng J, Li Q, Huang M, Liu X, Owusu K A, Liu Z and Mai L 2018 *Adv. Funct. Mater.* **28** 1802016
[27] Wang Z, Huang J, Guo Z, Dong X, Liu Y, Wang Y and Xia Y 2019 *Joule* **3** 1289
[28] Wu Y, Wang M, Tao Y, Zhang K, Cai M, Ding Y, Liu X, Hayat T, Alsaedi A and Dai S 2020 *Adv. Funct. Mater.* **30** 1907120
[29] Wan F, Zhang L, Wang X, Bi S, Niu Z and Chen J 2018 *Adv. Funct. Mater.* **28** 1804975
[30] Kang L, Cui M, Jiang F, Gao Y, Luo H, Liu J, Liang W and Zhi C 2018 *Adv. Energy Mater.* **8** 1801090
[31] Cheng X B, Zhang R, Zhao C Z and Zhang Q 2017 *Chem. Rev.* **117** 10403